# Theoretical Stability Analysis of Isolated Bidirectional Dual Full Bridge DC-DC Converter

K. Wu [1] C. W. de Silva [2] W. G. Dunford [1]

**Abstract–This paper presents a new method for theoretical stability analysis of a bidirectional dual full bridge DC-DC converter with triple phase-shift control. The developed approach is analytically sound and generally applicable when compared with the existing approaches, which are by and large based on computer simulation. The operating process of a bidirectional converter is multi-stage and nonlinear, which is explained by giving consideration to the control method that is used. Based on its working theory, the converter is separated into several stages. Equivalent circuits and state equations are built for each stage to determine the stability in each stage. Then, abrupt state changes and the response to infinite noise are analyzed for stage transitions. Next, the stability of the bidirectional converter is determined using the eigenvalue method. The analytical results are validated through computer simulation.**

**Keywords–Bidirectional isolated DC-DC converter, stability analysis, triple phase-shift control, equivalent circuits, state equations, eigenvalue method.**

## I. INTRODUCTION

In recent years, the development of high power and large power range isolated bidirectional dc-dc converters has become an important topic because of the requirements of electric automobile, uninterruptible power supply and aviation power system [1], [2], [4], [9]. An identical dual active full bridge converter with zero voltage switching (ZVS) can be used on both sides of the isolation transformer as shown in Fig. 1 [3, 5,14]. Stability is an important requirement in any practical engineering system [6-8]. Some parameters of a bidirectional converter may change arbitrarily, and it is important that converter operates properly under these conditions. This paper presents an effective approach, using the eigenvalue method, to determine the stability of a nonlinear bidirectional DC-DC converter when the parameters change arbitrarily. The novel approach of triple phase-shift control is used in this paper as it can improve system efficiency and adaptability to parameter changes.

This method developed in this paper may be used to study stability of other similar nonlinear time-varying circuitry as well. The organization of the rest of the paper is as follows. The problem addressed in the paper is described in detail in Section II. The stability analysis method used in the paper is described in Section III. The operation of the bidirectional dual full bridge converter with the novel triple phase-shift control is analyzed and the equivalent circuits are derived in Section IV. In Section V, the stability of the bidirectional converter is determined with the developed method, when the input voltage changes arbitrarily. The results obtained from the analysis are validated using simulations and discussed in Section VI. The main contributions of the paper are summarized in Section VII.

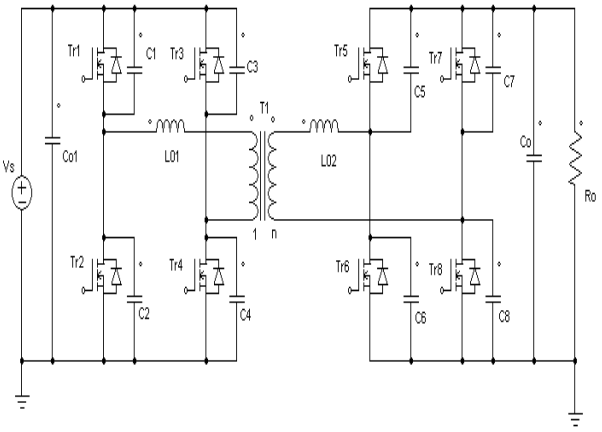


Fig. 1: The power circuit of the bidirectional converter.

## II. PROBLEM DESCRIPTION

*1. Statement of the Problem*

In power electronics, stability of a power converter is usually determined through simulation because it is nonlinear system whose stability analysis is quite difficult. This is especially true for high power zero voltage switching (ZVS) converters [10], [12]. However, the method of simulation is not always appropriate because simulation results only provide information under specific working conditions. When input voltage changes for some reason, the converter will work in a different state. It is impossible to simulate the infinite number of such working conditions that are possible. Analytical determination of stability analysis is more general, and is desired in this backdrop [17].

This paper presents an effective method to determine the stability of a bidirectional DC-DC converter with triple phase-shift control under possible input voltage changes. For this purpose, first a mathematical model has to be developed for the bidirectional converter with dual phase-shift control, which is a nonlinear system. Besides this, the input voltage change must be taken into account when determine its stability. The problem is exacerbated by the fact that the input voltage can change, and this change is unknown in general.

Although the problem of stability analysis can be difficult and complex, the periodic operation of a bidirectional converter can be analytically represented. The bidirectional converter is separated into several stages in one period, guided by results from computer simulation

The paper first received 30 Nov 2010 and in revised form 22 Apr 2013.
Digital Ref: APEJ-2013-07-312
[1] Department of Electrical and Computer Engineering, The University of British Columbia, Vancouver, BC, V6T 1Z4, Canada
[2] Department of Mechanical Engineering, The University of British Columbia, Vancouver, BC, V6T 1Z4, Canada
E-mail: wukuiyuan2010@hotmail.com

under normal conditions. An equivalent circuit is developed for every stage of operation by approximating the nonlinear power switches and diodes with linear ones; for example, replacing the power MOSFET with an on-resistance when it conducts and replacing the diodes with voltage sources of their conduction voltage values. In this manner, an approximately linear time-varying equivalent circuit model is established for each stage or sub-stage. According to the equivalent circuit, the approximately state equation can be built for each stage or sub-stage. This facilitates the stability analysis of the bidirectional converter in every stage and within the entire period of operation.

*2. Components in Power Circuit*

The components in the power circuit of the converter are identified below.

*L01*, *L02* ---- Two series inductors
*C1=C2=C3=C4=C5=C6=C7=C8* --- Eight snubber capacitors
*Co*, *Co1* ---Two large filter capacitors
*Ro* --- Forward load resistor

The parameters of the main transformer are as follows:

*Lp* ---Primary leakage inductance
*Ls* --- Secondary leakage inductance
*Rp* --- Primary winding resistance
*Rs*--- Secondary winding resistance
Turns ratio: 1: *n*

The parameters of the eight power MOSFETs are as follows:

*R1*, *R2*, *R3*, *R4*, *R5*, *R6*, *R7*, *R8* ---- On-resistance
*D1*, *D2*, *D3*, *D4*, *D5*, *D6*, *D7*, *D8* --- Anti-parallel diodes with power MOSFETs.

*3. Variables Used in the Paper*

*iap*, *ias* ---Power circuit primary current and secondary current of the transformer
*Vc1*, *Vc2*, *Vc3*, *Vc4*, *Vc5*, *Vc6*, *Vc7*, *Vc8* ---Voltages across the corresponding parallel capacitors.
*Vs* ---Input voltage
*Vo* ---Output voltage
$V_{D1}$, $V_{D2}$, $V_{D3}$, $V_{D4}$, $V_{D5}$, $V_{D6}$, $V_{D7}$, $V_{D8}$ ----Forward conduction voltages of anti-parallel diodes.

## III. Stability Analysis of Dual Full Bridge Converter

*1. The Method*

The bidirectional DC-DC converter has many nonlinear components, and is essentially a nonlinear system during its entire period of operation. However, it can be separated into several linear stages according to the simulation wave-forms under normal working conditions. The equivalent circuit and the corresponding state equations can be established for each stage. Using these state equations, stability can be analyzed for every stage. If the converter is stable in every stage and there is no abrupt state change at the interface of two stages, this converter will be stable during the entire working period. In this context, for analytical purposes, abrupt state change means an instantaneous change in the state variables at the interface of different stages.

Based on this idea, the forward bidirectional dual full bridge converter is separated into eight main stages for the purpose of theoretical analysis of its stability. There are no abrupt state changes during the transition between two stages because the two stages are connected with each other by the capacitor voltages and inductor currents. It is well known they cannot change abruptly. Therefore, the forward bidirectional dual full bridge converter with triple phase-shift control will be stable if it is stable in each stage. Only the forward response is considered in the present analysis. The stability of the backward bidirectional dual full bridge converter with triple phase-shift control can be analyzed similarly.

*2. Component Parameters in Power Circuit*

*L01*=7.3μH;
*C1=C2=C3=C4=C5=C6=C7=C8*=1nF;
*L02*=6.9μH;
*Co=Co1*=500μF;
*Ro*=40Ω;
*Lp*=0.6μH;
*Ls*=1μH;
*Rp*=7mΩ;
*Rs*=10mΩ;
*n*=7/2

The parameters of the 8 power switches are as follows:

*Tr1~Tr4*: On resistance: 5mΩ; Diode Voltage drop: 1V
*Tr5~Tr8*: On resistance: 23mΩ; Diode Voltage drop: 0.6V

## IV. Equivalent Circuits

The forward simulation wave-forms of the bidirectional converter with normal steady state operation are shown in Fig. 2. As shown, the triple phase-shift control method includes three phase-shifts. The first is the phase-shift between the primary control signal and the corresponding secondary control signal, for example, between *Vg1* and *Vg5*; the second is the phase-shift between the diagonal control signals in the primary power circuit, for example, between *Vg1* and *Vg4*; and the third is the phase-shift between the diagonal control signals in the secondary power circuit, for example, between *Vg5* and *Vg8*.

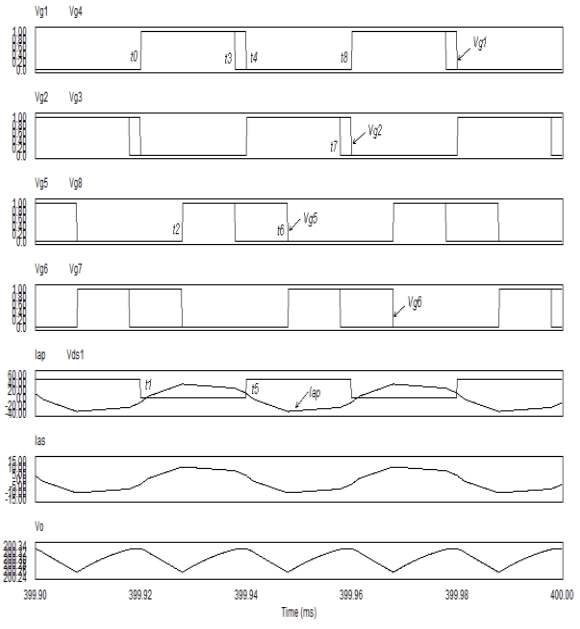

Fig. 2: Simulation wave forms of the forward bidirectional converter with triple phase-shift control.

The forward bidirectional dual full bridge converter is separated into eight stages in one period. Its operation and the equivalent circuit for every stage are described below.

*A. Stage 1 (t0~t1)*

Power switches *Tr1* and *Tr4* will turn on at "*t=t0*". Because the primary current is still negative during this period, the primary current will flow through *Tr4/Tr1* and the inductor energy flows back to the power source.

Because *Vg5*/*Vg8*/*Vg7* are equal to zero, *Tr5/Tr8/Tr7* are all in the "Off" state; *Vg6*=1, *Tr6* is "On". *Ias*<0 and secondary current flows through *Tr6/D7*. The inductor *L02* and output capacitor provide energy to the load. The output voltage reduces during this period. The equivalent circuit in this stage is given in Fig. 3.

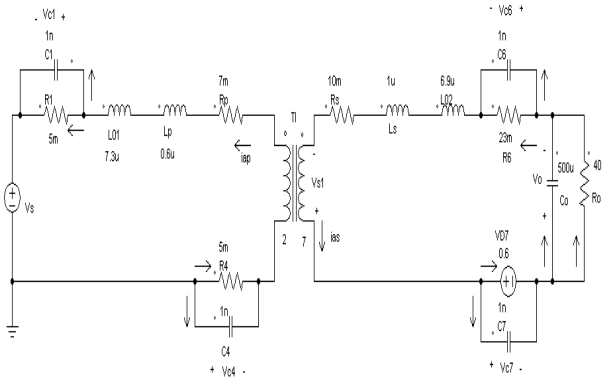


Fig. 3: Equivalent circuit in stage 1.

*B. Stage 2 (t1~t2)*

Because *Vg1*/ *Vg4* =1, power switches *Tr1* and *Tr4* are in "On" state in this period. Because the primary current is positive during this period, the primary current will flow through *Tr1/Tr4*, inductor *L01* and the transformer leakage inductance. The energy will transfer from the primary side to the secondary side.

Because *Vg5*/*Vg8*/*Vg7* are equal to zero, *Tr5/Tr8/Tr7* all are in the "Off" state; *Vg6*=1, *Tr6* is "On". *Ias*>0 and secondary current will charge capacitor *C7* and discharge capacitor *C8* until its voltage reduces to the forward conduction voltage of diode *D8*. The corresponding equivalent circuit is given in Fig. 4.

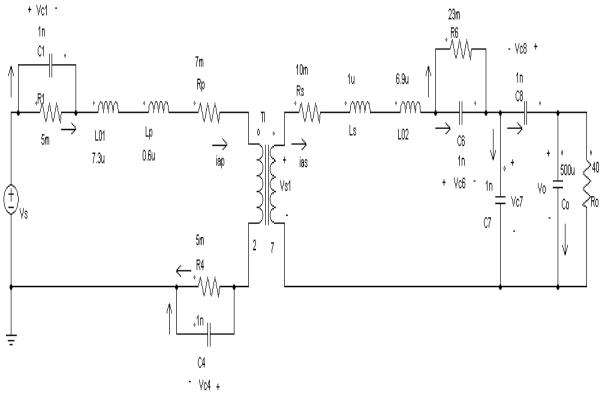


Fig. 4: *C8* discharging equivalent circuit in stage 2.

Then the current flows through Tr6/D8. The energy is stored in the secondary inductor *L02* and the leakage inductor because this is a freewheeling period with no power transfer to the load, in theory. Output capacitor provides energy to the load and the output voltage continues to reduce in this period. The equivalent circuit in this stage is given in Fig. 5.

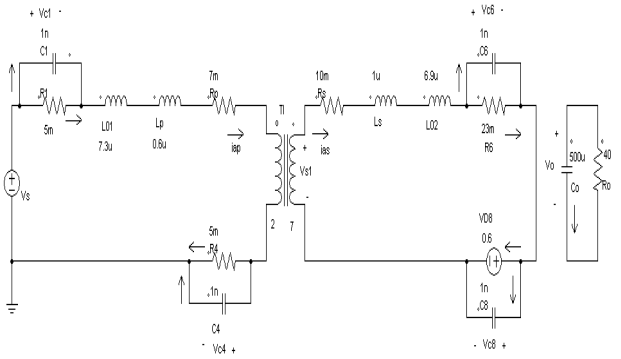


Fig. 5: Free-wheeling equivalent circuit in stage 2.

*Tr6* turns off just before *t2*. The secondary current will charge the snubber capacitor *C6* and discharge the snubber capacitor *C5*. During this very short period of transitional time, the secondary current flows through *D8* to charge and discharge the snubber capacitors. When *C5* is totally discharged (*Vds5*=0), the secondary current will flow through *D5/D8* and the energy will be transferred to the load. The corresponding equivalent circuits are shown in Fig. 6 and Fig. 7.

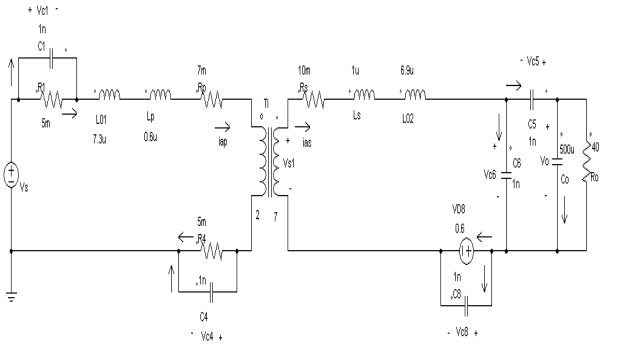


Fig. 6: Charge-discharge equivalent circuit in stage 2.

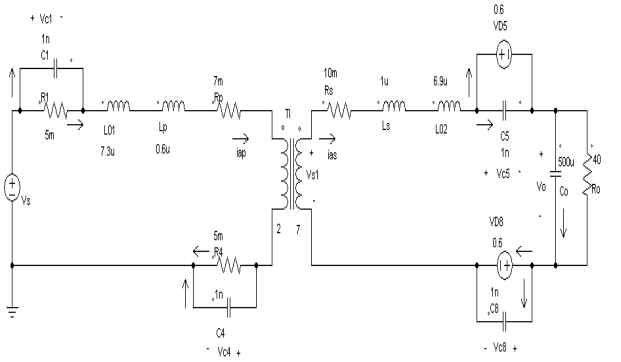


Fig. 7: Diode conduct equivalent circuit in stage 2.

*C. Stage 3 (t2~t3)*

The control signal *Vg5*/*Vg8*=1. The power switches *Tr5/Tr8* will turn on at *t2*. Because *Ias*>0 during this stage, the secondary side current will flow through *Tr5/Tr8* and transfer energy to the load. The output voltage will

increase. The equivalent circuit in this stage can be obtained as before, and is shown in Fig. 8.

*D. Stage 4 (t3~t4)*

Here *Vg4*/*Vg8*=0; so, *Tr4*/*Tr8* will turn off at $t_3$. For the primary side, *Tr4* turns off at $t_3$. The primary current will charge the snubber capacitor *C4* and discharge the snubber capacitor *C3*. When *C3* is completely discharged (*Vds3*=0), the primary current will flow through *Tr1*/*D3* and form a free-wheeling sub-stage. No power is transferred to the secondary side, in theory.

For the secondary side, the current *ias*>0. This indicates that *Tr5*/*D8* will continue to conduct in this period of time. The additional inductor *L02* and the secondary leakage inductance will provide energy transfer to the load. The output voltage will continue to increase in this stage. The corresponding equivalent circuits are shown in Fig. 9 and Fig. 10.

*Tr1* turns off just before $t_4$. The primary current will discharge the snubber capacitor *C2* and charge the snubber capacitor *C1*. During this very short transitional time, the current will flow through *D3* to charge and discharge the capacitors. When *C2* is completely discharged (*Vds2*=0), *D2* will conduct and form an energy feedback to the power source. This will make it feasible for *Tr2*/*Tr3* to turn on under ZVS. The corresponding equivalent circuits are shown in Fig. 11 and Fig. 12.

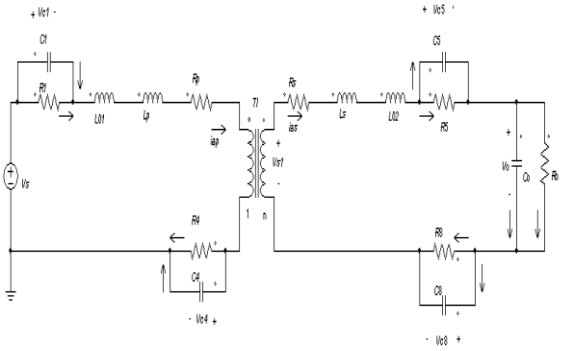

Fig. 8: Energy transfer equivalent circuit in stage 3.

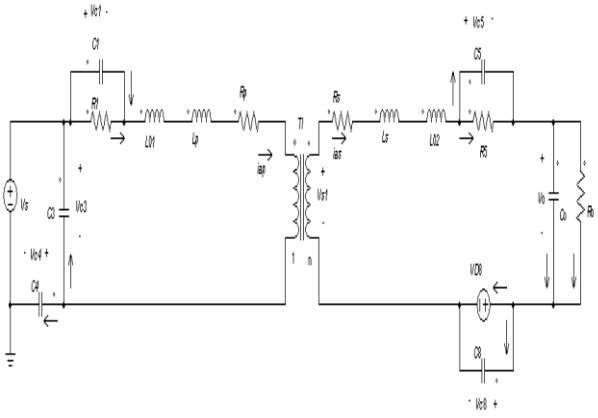

Fig. 9: *C3* discharge equivalent circuit in stage 4

*E. Stage 5 ( t4~t5)*

Because *Vg2*/*Vg3*=1, *Tr2/Tr3* will turn on at *t4*. *Tr1* turns off just before *t4*. The primary current will discharge the snubber capacitor *C2* and charge the snubber capacitor *C1*. During this short transitional period, the current will flow through *D3* to charge and discharge the capacitors. When *C2* is completely discharged (*Vds2*=0), *D2* will conduct and form an energy feedback to the power source. Therefore, *Tr2/Tr3* will turn on at *t4* under ZVS. Because the primary current *Iap*>0, the energy will feedback to the primary source in this stage.

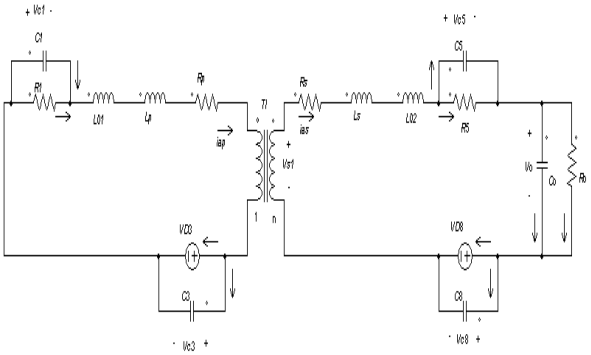

Fig. 10: Free-wheeling equivalent circuit in stage 4.

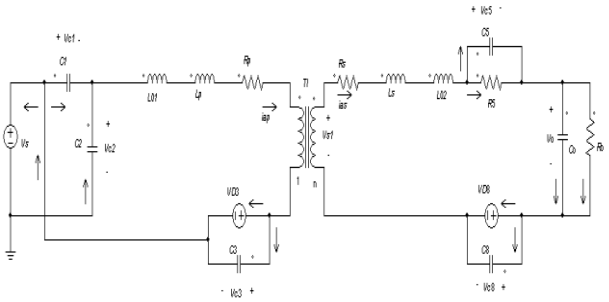

Fig. 11: *C2* discharge equivalent circuit in stage 4.

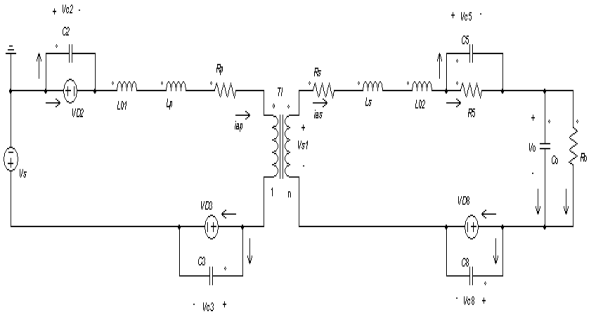

Fig. 12: Energy feedback equivalent circuit in stage 4.

For the secondary side, *Vg5*=1; so, *Tr5* is "On" in this stage. *Vg6*/*Vg7*/*Vg8*=0; so, *Tr6/Tr7/Tr8* all will be in the off state during this period of time. Because the secondary side current *Ias*>0, *Tr5/D8* will conduct in this period of time. The inductor *L02*, the secondary leakage inductor and the output capacitor together will provide energy to the load in this stage. The output voltage begins to reduce in this stage. According to this analysis, the equivalent circuits for this stage may be obtained as before.

*F. Stage 6 (t5~t6)*

Because *Vg2/Vg3*=1, *Tr2/Tr3* will be on in this stage. Because the primary current *Iap*<0, the energy will transfer to the secondary side again. For the secondary side, *Vg5*=1; so, *Tr5* is on state in this stage. *Vg6/Vg7/Vg8*=0; so, *Tr6/Tr7/Tr8* all will be in the off state during this period of time. Because the secondary side current *Ias*<0, the secondary current will charge the capacitor *C8* and discharge the capacitor *C7* until its

voltage reduces to the forward conduction voltage of diode *D7*. Then the current will flow through *Tr5/D7* in this period of time and form a freewheeling period with no energy transfer to the load, in theory, in this stage. The energy from the primary source is stored in *L02* and the leakage inductor. The output capacitor provides energy to the load and the output voltage will continue to reduce in this stage. The equivalent circuit can be obtained as bore, for this stage.

*G. Stage 7 (t6~t7)*

Because *Vg6/Vg7*=1, *Tr6/Tr7* will turn on at *t6*. *Vg5*=0; so, *Tr5* turns off just before *t6*. The secondary current will charge *C5* and discharge *C6*. During this very short of transitional time, the secondary current will flow through *D7* to charge and discharge the snubber capacitors. When *C6* is completely discharged (*Vds6*=0), *D6* will turn on and *D6/D7* will conduct to form ZVS and transfer energy to the load. Because the secondary side current *Ias<0*, *Tr6/Tr7* will conduct in this period of time and transfer energy to the load, and the output voltage will increase in this stage. The equivalent circuits in this stage can be obtained as before.

*H. Stage 8 (t7~t8)*

Because *Vg3*/*Vg7*=0 at t7, Tr3/Tr7 will turn off at *t7*. On the primary side, *Tr3* will turn off; and the primary current will charge *C3* and discharge *C4*. During this very short of transitional time, the primary current will flow through *Tr2* to charge and discharge the snubber capacitors *C3* and *C4*. When *C4* is completely discharged (*Vds4*=0), *D4* will turn on. *Tr2/D4* will conduct. This will form a freewheeling stage with no energy transfer to the secondary side theoretically. *Tr2* turns off just before *t8*. The energy stored in the additional inductor *L01* and the transformer leakage inductance will charge the snubber capacitor *C2* and discharge the snubber capacitor *C1*. During this very short period of transitional time, the primary current will flow through *D4* to charge and discharge the snubber capacitors. When *C1* is completely discharged (*Vds1*=0), then the primary current will flow through *D4/D1* and the inductor energy will flow back to the power source.

On the secondary side, *Tr6/D7* will continue to conduct during this period of time and transfer energy to the load. This is because the secondary side current *Ias*<0. The energy mainly comes from the stored energy of additional inductor *L02* and the leakage inductance. Output voltage will continue to increase in this stage. The corresponding equivalent circuits can be obtained as before, based on the analysis for this stage.

## V. Stability Analysis with Eigenvalue Method

Based on the equivalent circuits in each stage, the corresponding state equation can be built for this bidirectional DC-DC converter in each stage. The equivalent circuits are got by the analysis of the combination act of the input signal, output signal and control signal of this closed-loop converter. According to model identification [13], [16], the equivalent circuits in each stage are closed-loop models for this nonlinear DC-DC converter. The corresponding state equation will be a closed-loop state space model of this bidirectional converter in each linear stage. It can be used to determine the stability of this bidirectional converter in every linear stage directly.

*A. Stability Analysis in Stage $t_0$~$t_1$*

From the equivalent circuit of the converter, as shown in Fig.3, the state equations of the converter can be generated for this stage. For convenience, let:

$$V_{eq} = L01 + L_p + \frac{1}{n^2} L02 + \frac{1}{n^2} L_s$$

$$R_{eq} = R_p + \frac{1}{n^2} R_s$$

$$L_{eq} \frac{diap}{dt} = -R_{eq} i_{ap} - V_{c1} - V_{c4} - \frac{1}{n} V_{c6} - \frac{1}{n} V_o - \frac{1}{n} V_{D7} - V_s \quad (1)$$

$$C1 \frac{dV_{c1}}{dt} = i_{ap} - \frac{V_{c1}}{R_1}$$

$$C4 \frac{dV_{c4}}{dt} = i_{ap} - \frac{V_{c4}}{R_4}$$

$$C6 \frac{dV_{c6}}{dt} = \frac{1}{n} i_{ap} - \frac{V_{c6}}{R_6}$$

$$C_o \frac{dV_o}{dt} = \frac{1}{n} i_{ap} - \frac{V_o}{R_o}$$

Substitute the corresponding values into these state equations. The complete stat equations are obtained, as given below.

$$\frac{di_{ap}}{dt} = 915.26 i_{ap} - 117096 V_{c1} - 117096 V_{c4} - 33456 V_{c6} - 33456 V_o - 33456 V_{D7} - 117096 V_s$$

$$\frac{dV_{c1}}{dt} = 10^9 i_{ap} - 2 \cdot 10^{11} \cdot V_{c1} \quad (2)$$

$$\frac{dV_{c4}}{dt} = 10^9 i_{ap} - 2 \cdot 10^{11} \cdot V_{c4}$$

$$\frac{dV_{c6}}{dt} = 2.86 \cdot 10^8 i_{ap} - 4.35 \cdot 10^{10} \cdot V_{c6}$$

$$\frac{dV_o}{dt} = 571 i_{ap} - 50 \cdot V_o$$

Therefore, the closed-loop state space model of this converter during this stage may be expressed as:

$$\dot{x} = Ax + Bu$$
$$y = Cx \quad (3)$$

Where

$$x=[i_{ap}\quad V_{c1}\quad V_{c4}\quad V_{c6}\quad V_o]^T, u=[V_{D7}\quad V_s]^T, y=V_o$$

The eigenvalues of the system matrix ***A*** for the present converter in this stage are given below:

$$\begin{aligned} s1&=-43499999780\\ s2&=-1178.092+4222.65i\\ s3&=-1178.092-4222.65i\\ s4&=-1.999\cdot10^{11}\\ s5&=-2.0\cdot10^{11} \end{aligned} \tag{4}$$

Therefore, the converter is state asymptotically stable in this stage. Its stability is irrelevant to the input signal $V_S$ and the forward diode voltage $V_{D7}$ because they only influence the input distribution matrix and do not influence the system matrix.

*B. Stability Analysis in Stage $t_1$~$t_2$*

From the previous analysis of the working process of the converter, it is seen that there are three sub-stages and corresponding three equivalent circuits in this stage. The stability of the converter can be analyzed in these three sub-stages with their equivalent circuits, one by one.

*(1) Sub-stage of Charge-discharge of C7 and C8*

According to the equivalent circuit of the converter shown in Fig.4, the corresponding state equations are given below:

$$\begin{aligned} L_{eq}\frac{di_{ap}}{dt}&=-R_{eq}i_{ap}-V_{c1}-V_{c4}-\frac{1}{n}V_{c6}-\frac{1}{n}V_{c7}+V_s\\ C1\frac{dV_{c1}}{dt}&=i_{ap}-\frac{V_{c1}}{R1}\\ C4\frac{dV_{c4}}{dt}&=i_{ap}-\frac{V_{c4}}{R4}\\ C6\frac{dV_{c6}}{dt}&=\frac{1}{n}i_{ap}-\frac{V_{c6}}{R6}\\ \frac{dV_{c7}}{dt}&=\frac{(C8+Co)i_{ap}}{n(C7\cdot C8+Co\cdot C8+Co\cdot C7)}\\ &\quad-\frac{C8(V_{c7}+V_{c8})}{Ro(C7\cdot C8+Co\cdot C8+Co\cdot C7)}\\ \frac{dV_{c8}}{dt}&=\frac{-Coi_{ap}}{n\left(C7\cdot C8+Co\cdot C8+Co\cdot C7\right)}\\ &\quad-\frac{C7\left(V_{c7}+V_{c8}\right)}{Ro\left(C7\cdot C8+Co\cdot C8+Co\cdot C7\right)}\\ V_o&=V_{c7}+V_{c8} \end{aligned} \tag{5}$$

Substitute the corresponding component values into these state equations, the final state equations for the converter in this sub-stage can be obtained, as given below:

$$\begin{aligned} \frac{d_{iap}}{dt}&=-915.26i_{ap}-117096V_{c1}-117096V_{c4}\\ &\quad-33456V_6-33456V_{c7}+117096V_s\\ \frac{dV_{c1}}{dt}&=10^9 i_{ap}-2\cdot10^{11}\cdot V_{c1}\\ \frac{dV_{c4}}{dt}&=10^9 i_{ap}-2\cdot10^{11}\cdot V_{c4}\\ \frac{dV_{c6}}{dt}&=2.86\cdot10^8\cdot i_{ap}-4.35\cdot10^{10}\cdot V_{c6}\\ \frac{dV_{c7}}{dt}&=1.43\cdot10^8\cdot i_{ap}-25\cdot V_{c7}-25\cdot V_{c8}\\ \frac{dV_{c8}}{dt}&=-1.43\cdot10^8\cdot i_{ap}-25\cdot V_{c7}-25\cdot V_{c8}\\ V_o&=V_{c7}+V_{c8} \end{aligned} \tag{6}$$

Therefore, the closed-loop state space model of this converter during this stage can be expressed as:

$$\begin{aligned} \dot{x}&=Ax+Bu\\ y&=Cx \end{aligned} \tag{7}$$

where

$$x=\left[i_{ap}\quad V_{c1}\quad V_{c4}\quad V_{c6}\quad V_{c7}\quad V_{c8}\right]^T, u=\left[V_{D7}\quad V_5\right]^T, y=V_0$$

The eigenvalues of the system matrix in this sub-stage are:

$$\begin{aligned} s1&=-1153.09+2187282.95i\\ s2&=-1153.09-2187282.95i\\ s3&=-43499999780\\ s4&=-1.999\cdot10^{11}\\ s5&=-2.0\cdot10^{11}\\ s6&=-50 \end{aligned} \tag{8}$$

All eigenvalues have negative real parts. Hence, the converter in this sub-stage is state asymptotically stable. There is no abrupt change in state from stage 1 to stage 2. The converter does not receive infinite noise.

*(2) Sub-stage of Free Wheeling in Stage 2*

According to the equivalent circuit of the converter in the freewheeling stage, as shown in Fig.5, the corresponding state equation for the converter during the present sub-stage can be obtained as follows:

$$\begin{aligned} L_{eq}\frac{di_{ap}}{dt}&=-R_{eq}i_{ap}-V_{c1}-V_{c4}-\frac{1}{n}V_{c6}-\frac{1}{n}V_{D8}+V_S\\ C1\frac{dV_{C1}}{dt}&=i_{ap}-\frac{V_{c1}}{R_1}\\ C4\frac{dV_{C4}}{dt}&=i_{ap}-\frac{V_{c4}}{R_4}\\ C6\frac{dV_{C6}}{dt}&=\frac{1}{n}i_{ap}-\frac{V_{c6}}{R_6}\\ Co\frac{dV_o}{dt}&=-\frac{V_o}{R_o} \end{aligned} \tag{9}$$

Substitute the corresponding component values into these state equations. Then, the complete state equations for the present converter in this sub-stage can be gotten as follows:

$$\begin{aligned}
\frac{di_{ap}}{dt} &= 915.26\cdot i_{ap} - 117096\cdot V_{c1} - 117096\cdot V_{c4} \\
&\quad - 33456\cdot V_{c6} - 33456\cdot V_{D8} + 117096\cdot V_S \\
\frac{dV_{c1}}{dt} &= 10^9 i_{ap} - 2\cdot 10^{11}\cdot V_{c1} \\
\frac{dV_{c4}}{dt} &= 10^9 i_{ap} - 2\cdot 10^{11}\cdot V_{c4} \\
\frac{dV_{c6}}{dt} &= 2.86\cdot 10^2\cdot i_{ap} - 4.35\cdot 10^{10}\cdot V_{c6} \\
\frac{dV_{c1}}{dt} &= -50V_o
\end{aligned} \tag{10}$$

Therefore, the closed-loop state space model of the present converter during the considered sub-stage may be expressed as:

$$\begin{aligned}
\dot{x} &= Ax + Bu \\
y &= Cx
\end{aligned} \tag{11}$$

where

$$x = \begin{bmatrix} i_{ap} & V_{c1} & V_{c4} & V_{c6} & V_o \end{bmatrix}^T, u = \begin{bmatrix} V_{D8} & V_S \end{bmatrix}^T, y = V_0$$

The eigenvalues of the system matrix in this sub-stage are given by:

$$\begin{aligned}
s1 &= -2306.18 \\
s2 &= -1.999\cdot 10^{11} \\
s3 &= -43499999780 \\
s4 &= -2.0\cdot 10^{11} \\
s5 &= -50
\end{aligned} \tag{12}$$

All eigenvalues have negative real parts. Hence, the converter in this sub-stage is state asymptotically stable. There is no abrupt change in the state variables between these two sub-stages. Also, there is no infinite noise to the converter.

The stability of the converter in the other stages can be analyzed similarly. It can be established that the bidirectional converter is asymptotically stable in every stage. There are no state abrupt changes between stages or sub-stages. This means there is no infinite noise into the converter. Therefore, this converter is stable during the entire working period.

## VI. Simulation Studies and Discussion

Section V presented an effective method to establish the stability of a bidirectional converter under triple phase-shift control, when the input voltage changes. The changes of the three phase shifts due to a change in the input voltage will only change the time duration of some working stages. Hence, the general equivalent circuit and the state equations in every stage will remain the same. If the converter is stable in these stages, it will remain stable when the time durations of the stages change. This can be validated by computer simulation.

Fig.13 is got by simulating the bidirectional converter with triple phase-shift control when the input voltage changes from 48V to 55V. There are 6 stages in one period at present. By comparing Fig.13 with Fig.2, it is seen that two stages disappear and the time duration of the other stages becomes different when the input voltage changes. But the output voltage will remain very close to 200V with a small error, by adjusting the feedback resistance values to 100kΩ/2.28kΩ, and the bidirectional converter is BIBO stable. This result validates the eigenvalue method as proposed in this paper, for establishing the stability of a bidirectional converter with triple phase-shift control when only the input voltage changes. If the converter is unstable, however, a different topology should be considered [11], [15], [18]. Fig.2 and Fig.13 are obtained through simulation with PSIM.

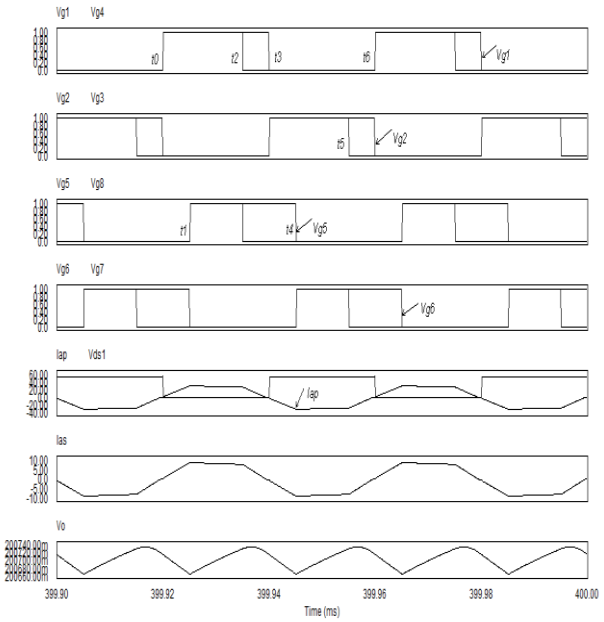


Fig. 13: Simulation results of forward bidirectional converter with triple phase-shift control when input voltage changes.

There is a limit to the application of the present method of stability analysis. If the system parameters change, the present method is not valid. Then, the converter is approximately linear and time variant in every stage, and the matrix ***A*** is a function of time. The eigenvalue method cannot be applied.

## VII. Conclusion

This paper presented a new method to theoretically analyze the stability of a nonlinear bidirectional dual full bridge DC-DC converter with triple phase-shift control. First, the nonlinear converter was separated into several linear stages in one period, and equivalent circuits and the corresponding state equations were determined for each stage. It was proved that the converter was stable in every stage and there were no abrupt change of state between two neighboring stages or sub-stages. This established that the converter would remain stable during the transition from one stage to the next. Then, it was shown that that the converter would be stable in the entire period. The

results were validated through computer simulation.

## REFERENCES


[1] A. Xu and S. Xie, "A Multipulse-Structure-Based Bidirectional PWM Converter for High-Power Applications," *IEEE Trans. Power Electron*., vol.24, no.5, pp. 1233-1242, May 2009.

[2] H.J. Chiu and L.W. Lin, "A bidirectional DC-DC converter for fuel cell electric vehicle driving systems," *IEEE Trans. Power Electron*., vol. 21, no. 4, pp. 950-958, July 2006.

[3] S. Inoue and H. Akagi, "A Bidirectional DC-DC Converter for an Energy Storage System with Galvanic Isolation," *IEEE Trans. Power Electron*., vol.22, no.6, November 2007.

[4] H. Bai and C. Mi, "Eliminate Reactive Power and Increase System Efficiency of Isolated Bidirectional Dual Active Bridge DC-DC Converters Using Novel Dual Phase Shift Control," *IEEE Trans. Power Electron*., vol.23, no.6, November 2008.

[5] G.G. Oggier, G.O. Garcia and A.R. Oliva, "Switching Control Strategy to Minimize Dual Active Bridge Converter Losses," *IEEE Trans. Power Electron*., vol.24, no.7, pp. 1826-1838, July 2009.

[6] G. C. Goodwin, S. F. Graebe, and M. E. Salgado, Control System Design, Prentice Hall of India, 2006.

[7] P. J. Antsaklis and A. N. Michel, A Linear Systems Primer, Birkhäuser, Boston, MA, 2007.

[8] C.W. de Silva, Modeling and Control of Engineering Systems, Boca Raton, FL: CRC Press/Taylor & Francis, 2009.

[9] D.H. Xu, C.H. Zhao and H. F. Fan, "A PWM plus phase-shift control bidirectional DC-DC converter," *IEEE Trans. Power Electron*., vol. 19, no. 3, pp. 666-675, May 2004.

[10] L. Zhu, "A novel soft-commutating isolated boost full bridge ZVS-PWM dc-dc converter for bidirectional high power applications," *IEEE Trans. Power Electron*., vol. 21, no.2, pp. 422-429, March, 2006.

[11] Y.V. Hote, D.R. Choudhury, and J.R.P. Gupta, "Robust Stability Analysis of the PWM Push-Pull DC-DC Converter," *IEEE Trans. Power Electron*., vol.24, no.10, pp.2353-2356, Oct. 2009.

[12] K. Wu and W. G. Dunford, "An Unusual Full Bridge Converter to Realize ZVS in Large Load Scope," *Asian Power Electronics Journal*, vol. 2, no. 1, pp. 66-71, Apr. 2008.

[13] V. Valdivia, A. Barrado, A. Laazaro, P. Zumel, C. Raga and C. Fernandez, "Simple Modeling and Identification Procedures for Black-Box Behavioral Modeling of Power Converters Based on Transient Response Analysis," *IEEE Trans. Power Electron*., vol.24, no.12, pp. 2776-2790, Dec. 2009.

[14] F. Krismer and J.W. Kolar, "Accurate Small-Signal Model for the Digital Control of an Automotive Bidirectional Dual Active Bridge," *IEEE Trans. Power Electron*., vol.24, no.12, pp. 2756-2768, Dec. 2009.

[15] L. Huber, B.T. Irving and M.M. Jovanoic, "Review and Stability Analysis of PLL-Based Interleaving Control of DCM/CCM Boundary Boost PFC Converters," *IEEE Trans. Power Electron*., vol.24, no.8, pp. 1992-1999, Aug. 2009.

[16] S. Karagol and M. Bikdash, "Generation of Equivalent-Circuit Models From Simulation Data of a Thermal System," *IEEE Trans. Power Electron*., vol.25, no.4, pp. 820-828, April 2010.

[17] W. Chen, X. Ruan, H. Yan, and C.K. Tse, "DC/DC Conversion Systems Consisting of Multiple Converter Modules: Stability, Control, and Experimental Verifications," *IEEE Trans. Power Electron*., vol.24, no.6, pp. 1463-1474, June 2009.

[18] J. Morroni, R. Zane, and D. Maksimovic, "An Online Stability Margin Monitor for Digitally Controlled Switched-Mode Power Supplies," *IEEE Transactions on Power Electronics*, vol.24, no.11, pp. 2639-2648, Nov. 2009.


## BIOGRAPHIES

**Kuiyuan Wu** received the B.S. degree from Southwest Jiao Tong University, China (1990); M.S. degrees from Chinese Academy of Sciences, Beijing, China (1997); and University of British Columbia, Canada (2008); and PhD degree from University of British Columbia, Vancouver, Canada (2012), all in electrical engineering. From 2009 to 2010, he was with Alpha Technologies Ltd. His current research interests include the combination of power electronics with advanced control theory, novel control method and novel power converter development, especially isolated bidirectional DC-DC converters, active power factor correctors, high power ZVS power supplies and high frequency inverter type resistance welding machines.

**Clarence W. de Silva** is a Fellow of: ASME, IEEE, Canadian Academy of Engineering, and Royal Society of Canada, and a distinguished Visiting Fellow of the Royal Academy of Engineering. He received Ph.D. degrees from Massachusetts Institute of Technology (1978); and University of Cambridge, U.K. (1998); and honorary D.Eng. degree from University of Waterloo, Canada (2008). A Professor of Mechanical Engineering and NSERC-BC Packers Chair holder in Industrial Automation, at the University of British Columbia, Vancouver, Canada since 1988, he currently occupies the Tier 1 Canada Research Chair in Mechatronics & Industrial Automation. He has authored 20 books and over 400 papers, approximately half of which are in journals. His recent books published by Taylor & Francis/CRC are: *Mechatronics—A Foundation Course* (2010); *Modeling and Control of Engineering Systems* (2009); *Sensors and Actuators—Control System Instrumentation* (2007); *VIBRATION—Fundamentals and Practice, 2nd Ed.* (2007); *Mechatronics—An Integrated Approach* (2005); and by Addison Wesley: *Soft Computing and Intelligent Systems Design—Theory, Tools, and Applications* (with F. Karray, 2004).

**William G. Dunford** received the B.S. and M.S. degrees from Imperial College, London, U.K. and the Ph.D. degree from the University of Toronto, Toronto, ON, Canada, all in electrical engineering. He has also been a faculty member of both institutions and is currently a faculty and Senate member of the University of British Columbia, Vancouver, BC, Canada. His industrial experience includes positions at the Royal Aircraft Establishment (now Qinetiq), Schlumberger and Alcatel. He has had a long term interest in photovoltaic powered systems and is also involved in projects in the automotive and distributed systems areas. Dr. Dunford has served in various positions on the Advisory Committee of the IEEE Power Electronics Society and chaired PESC in 1986 and 2001.